EFFECTS OF TEMPERATURE-DEPENDENT VISCOSITY VARIATIONS ON FULLY DEVELOPED LAMINAR FORCED CONVECTION IN A CURVED DUCT

Cláudia Regina de Andrade - claudia@mec.ita.cta.br
Edson Luiz Zaparoli - zaparoli@mec.ita.cta.br
Instituto Tecnológico de Aeronáutica – Departamento de Energia – IEME
Pça Marechal Eduardo Gomes, 50 – Vila das Acácias – 12228-900 – São José dos Campos – SP - Brasil

Abstract. *For most liquids the specific heat and thermal conductivity are almost independent from temperature, but the viscosity decreases significantly with it. A fully developed laminar water flow in a curved duct with temperature-dependent viscosity is analyzed in this work. The mass, momentum and energy conservation equations are numerically solved by the finite element method. Both heating and cooling of the water flow is studied. The secondary flow induced by the curvature effects increases the heat transfer rate in comparison with the straight ducts but the velocity and temperature profiles are distorted when the effects of temperature-varying viscosity are included. The Nusselt number obtained when the fluid is cooled with variable viscosity assumption are lower than the constant properties results due to the increase of the viscosity values at the inner points of the curved tube that reduces the secondary flow effect. The friction factor results also show a marked dependence on the viscosity variations in the coil tube cross-section.*

Key words: *Temperature-Dependent Viscosity, Curved Duct, Coil tube, Dean Number.*

1. INTRODUCTION

Laminar flow heat transfer in straight circular ducts with constant fluid properties was extensively investigated by Shah and London (1978). The temperature-varying property problem is complex due to the fact that fluid properties behave differently with temperature.

For *gases*, the density varies inversely with the first power of the absolute temperature but the specific heat varies only slightly with temperature. Furthermore, the viscosity and thermal conductivity increase as about 0.8 power of the absolute temperature. The Prandtl number, however, is practically independent from the temperature.

On the other hand, for most *liquids* the specific heat and thermal conductivity are almost independent from temperature, but the viscosity decreases significantly with it. Besides, the Prandtl number of liquids (oils, water) varies markedly with the temperature.

In the previous literature (Herwig, 1985; Etemad and Mujumdar, 1995), the effect of temperature-varying properties is often analyzed by approximate concepts like “property ratio method” or “reference temperature method”. These two schemes provide a correction for the constant-property results but according to Herwig and Klemp (1988), these methods were proposed for standard cases as pipe and boundary layer flow problems.

Harms et al. (1998) reviewed different models used to account the temperature-varying behavior of viscous liquids. The authors showed that these correlations provide reasonable predictions for many fluids but they are not valid over a large range of heating and cooling conditions or different geometries.

The effects of temperature-dependent viscosity variations were primarily focused on the circular tube geometry by Bergles (1983), neglecting the curvature effects. The first analytical investigation on flow in a coil tube was performed by Dean (1927), considering only constant properties. These results showed that the centrifugal forces induce a secondary circulation, represented by two vortices perpendicular to the main axial flow.

At this context, the purpose of this work is to analyze the influence of temperature-dependent viscosity variations on fully developed laminar forced convection considering the curvature effects. Both heating and cooling of the water flow in a coil tube is studied, showing that the friction factor and the Nusselt number results are dependent of the temperature-varying viscosity.

2. PROBLEM FORMULATION

Steady-state laminar incompressible water-flow in a curved duct is analyzed using a toroidal coordinate system showed in Fig.1. The flow is both hydrodynamically and thermally fully developed, with negligible viscous dissipation and axial conduction. All fluid properties are considered constant, with the exception of the viscosity in the coil tube cross-section. The temperature-varying viscosity $\mu(T)$ of the water is calculated by an extension of the Arrhenius model (Harms et. al, 1998) as follow:

$$ln(\mu) = C_0 + C_1 T + C_2 T^2 + C_3 T^3 + C_4 T^4 + C_5 T^5 \tag{1}$$

where T is the temperature field and C_n (n = 1, 2, 3 4, and 5) are constants determined by a polynomial over the water-viscosity data provided by Incropera and DeWitt (1981).

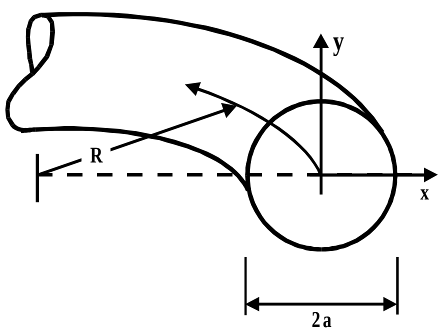

R = duct curvature radius and
a= duct cross-section radius

Figure 1. Circular curved duct in a toroidal coordinate system:

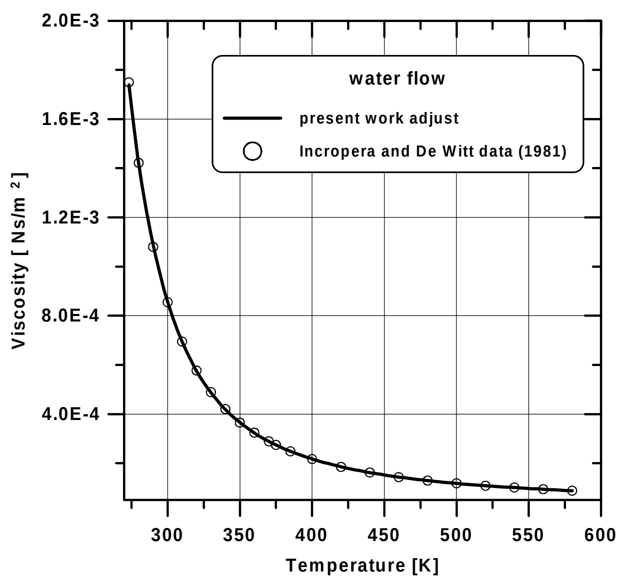

Figure 2. The temperature-varying viscosity for the water

Fig. 2 shows the water-viscosity distribution as a function of temperature resulting from Eq.1.

The fully developed flow and the constant axial temperature gradient assumptions result in the following conditions for velocity and temperature profiles are:

$$\frac{\partial u}{\partial z} = \frac{\partial v}{\partial z} = \frac{\partial w}{\partial z} = 0 \;\; ; \;\; \frac{\partial T}{\partial z} = \frac{dT_w}{dz} = \frac{dT_b}{dz} = \text{constant.}$$

where: z is the horizontal axial coordinate (main flow), w is the velocity component in the z direction, u and v are the velocity components in the transversal section (secondary flow), T_w is the wall temperature and T_b is the bulk mean temperature. The total pressure field P'(x, y, z) is decoupled in an axial contribution and in a part corresponding to the transversal one as:

$$P'(x,y,z) = \overline{P}(z) + P(x,y) \tag{2}$$

The governing equations (continuity, energy, x, y and z momentum equations) are represented by:

$$\frac{\partial u}{\partial x} + \frac{\partial v}{\partial y} + \frac{u}{R}\left[\frac{1}{1+(x/R)}\right] = 0 \tag{3}$$

$$\rho\left(u\frac{\partial u}{\partial x} + v\frac{\partial u}{\partial y} - \frac{w^2}{R(1+x/R)}\right) = -\frac{\partial P}{\partial x} + \frac{1}{(x+R)}\frac{\partial}{\partial x}\left[(x+R)\left(2\mu\frac{\partial u}{\partial x}\right)\right] - \frac{(2\mu u)}{(x+R)^2} + \frac{\partial}{\partial y}\left[\mu\left(\frac{\partial v}{\partial x} + \frac{\partial u}{\partial y}\right)\right] \tag{4}$$

$$\rho\left(u\frac{\partial v}{\partial x} + v\frac{\partial v}{\partial y}\right) = -\frac{\partial P}{\partial y} + \frac{1}{(x+R)}\frac{\partial}{\partial x}\left[\mu(x+R)\left(\frac{\partial v}{\partial x} + \frac{\partial u}{\partial y}\right)\right] + \frac{\partial}{\partial y}\left(2\mu\frac{\partial v}{\partial y}\right) \tag{5}$$

$$\rho\left[u\frac{\partial w}{\partial x} + v\frac{\partial w}{\partial y} + \frac{uw}{(x+R)}\right] = -\frac{1}{(x+R)}\frac{\partial \overline{P}}{\partial z} + \frac{1}{(x+R)^2}\frac{\partial}{\partial x}\left\{(x+R)^3\left[\mu\frac{\partial}{\partial x}\left(\frac{w}{x+R}\right)\right]\right\} + \frac{\partial}{\partial y}\left(\mu\frac{\partial w}{\partial y}\right) \tag{6}$$

$$u\frac{\partial T}{\partial x} + v\frac{\partial T}{\partial y} + \frac{w}{(1+x/R)}\frac{dT_b}{dz} = \frac{k}{\rho\, C_p}\left[\nabla^2 T + \frac{1}{R(1+x/R)}\frac{\partial T}{\partial x}\right] \tag{7}$$

with R equal to the duct curvature radius, ρ the fluid density, μ the fluid viscosity, C_p the fluid constant pressure specific heat and k the fluid thermal conductivity. Starting from the fluid properties the Prandtl number (Pr) can be defined as:

$$Pr = \frac{\mu\, Cp}{k} \tag{8}$$

The boundary conditions for the problem are:

$$u = v = w = 0 \;\text{ and }\; T = T_w \;\text{ at }\; \sqrt{x^2 + y^2} = a \;\text{ (see Fig. 1)} \tag{9}$$

After numerically determining the axial velocity (w) and the temperature field (T), the average velocity (w_m) and the Reynolds number (Re) were calculated as:

$$w_m = \frac{1}{A}\int w\, dA \quad \text{and} \quad Re = \left(\frac{\rho\, w_m\, D_h}{\mu}\right) , \tag{10}$$

where A is the duct cross-section area and D_h is the hydraulic diameter given by:

$$D_h = 2\, a \tag{11}$$

The Dean number (De) and the duct curvature ratio (RC) are calculated as follows:

$$De = Re\sqrt{\frac{D_h}{R}} \quad \text{and} \quad RC = \frac{R}{D_h} \tag{12}$$

The Nu (Nusselt number) and fRe (friction coefficient and Reynolds number product) are:

$$Nu = \frac{h\, D_h}{k} \quad \text{and} \quad f\, Re = \left(\frac{-2\, D_h\, (d\overline{P}/dz)}{\rho\, (w_m)^2}\right) Re \tag{13}$$

where the convection coefficient h is defined as:

$$h = \frac{q_{wm}}{(T_w - T_b)}, \quad q_{wm} = \frac{(dT_b/dz)\, \rho\, C_p w_m}{(1 + x/R)}\left[\frac{(a \cdot b)}{2\, (a+b)}\right] \tag{14}$$

In the case of a straight tube, some studies using *the property ratio method* (Kakaç, 1987) established a correlation for the Nusselt number and friction factor to correct the temperature-dependent viscosity variations. For laminar flow of *liquids* these correlations are:

$$Nu_{var} = Nu_{cte}\left(\frac{\mu_{tb}}{\mu_{tw}}\right)^{0,14} \quad \text{and} \quad f_{var} = f_{cte}\left(\frac{\mu_{tb}}{\mu_{tw}}\right)^{m} \tag{15}$$

with m = -0,58 for heating and m =-0,50 for cooling condition. The subscripts "*var*" and "*cte*" refer to variable and constant-viscosity, respectively. The sub-indices "*tb*" and "*tw*" are related to the absolute bulk mean and wall temperatures.

3. NUMERICAL SOLUTION

Firstly, by combining Eq. (4) and Eq. (5) a Poisson equation was derived to impose a mass conserving flow. So, the system of partial differential equations represented by the equations (4) to (7) and the Poisson equation were discretized applying the Galerkin finite elements technique. An unstructured mesh with triangular elements of six nodes and second-degree interpolation polynomials were used in the numerical solution. The system of resultant algebraic equations was solved by an iterative procedure in a non-segregated way, combining the Conjugated Gradient and Newton-Raphson methods. It was also used the *PDease®* program that provides an adaptive scheme with successive mesh refinement. This resource was applied in the more intense gradient regions and to capture the secondary flow effects (see Fig. 3b) induced by the centrifugal force. Fig. 3a presents the curved duct cross-section and an intermediary mesh in the solution process.

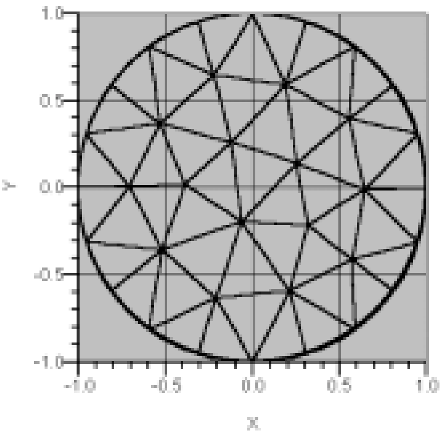

Figure 3a. Computational domain and an intermediary mesh in the solution process

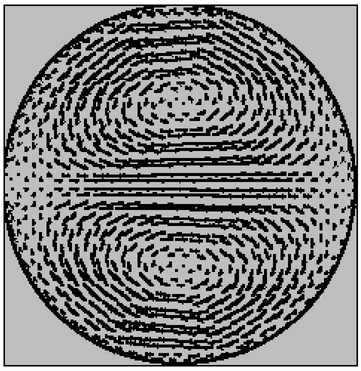

Figure 3b. Secondary flow in the curved tube cross-section at Dean number = 30

4. RESULTS AND DISCUSSION

4.1 Straight tube results

To calibrate the numerical code, the Nusselt number and the friction factor results obtained with variable-viscosity were compared with the literature correlations indicated by Eq. 15. In this method, the viscosity variations are corrected by the following ratio: μ_{tb}/μ_{tw} (viscosity at the mean bulk temperature to viscosity at the wall temperature). These comparisons are presented in Figs. 4 and 5 for the case of laminar water flow in a straight tube.

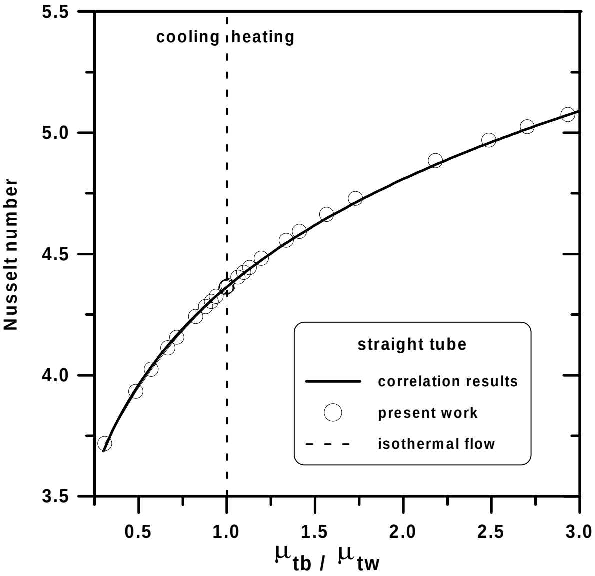

Figure 4. Nusselt number for the straight tube as a function of the viscosity ratio

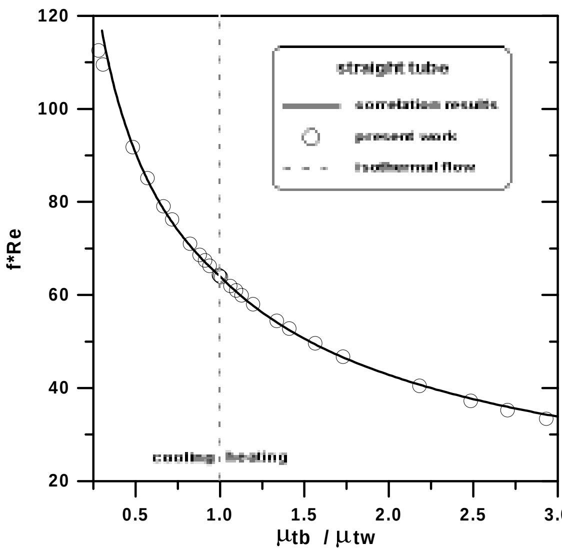

Figure 5. Friction factor for the straight tube as a function of the viscosity ratio

It is verified that in the range 0.3 < μ_{tb}/μ_{tw} < 3.0 (liquid water) the property ratio method and the solution of this work have a good agreement for both *Nu* and *fRe* results.

Figs. 4 and 5 show that for the isothermal condition ($\mu_{tb}/\mu_{tw} = 1$), the Nusselt number and friction factor results coincide with the constant property values (*Nu* = 4.364 and *fRe* = 64).

When water is cooled, the wall temperature (T_w) is smaller than the bulk mean temperature (T_b). Then, the viscosity value at the wall temperature is greater than the mean bulk temperature one and the *Nu* value decreases (Fig. 4) in comparison with the constant property value. On other hand, Fig. 5 shows that, under cooling conditions, the friction factor elevates because the viscosity decreases with the fluid temperature elevation increasing its viscosity close to the wall.

At heating-water ($T_w > T_b$) the viscosity value at wall temperature is smaller than the bulk mean temperature one. So, the Nusselt number increases (Fig. 4) and the *fRe* (Fig. 5) decays in comparison with the constant-properties values.

4.2 Curved duct results

The numerical simulations with constant-properties and variable-viscosity assumptions were carried out varying the Dean number in the range 2 < *De* < 200. The duct curvature ratio (Eq. 12) was maintained constant. Both heating and cooling of the laminar water flow in a curved duct were considered, with T_w = 350 K. The dT_b/dz value (see Eq. 7) was adjusted to obtain a bulk temperature $T_b = T_w + 35$ K for cooling-water and $T_b = T_w - 35$ K for heating-water conditions. In this temperature range, water still is in a liquid state.

The Dean number (*De*) influence on the temperature distribution at the curved tube cross-section is shown in Fig. 6, under cooling condition ($T_w < T_b$).

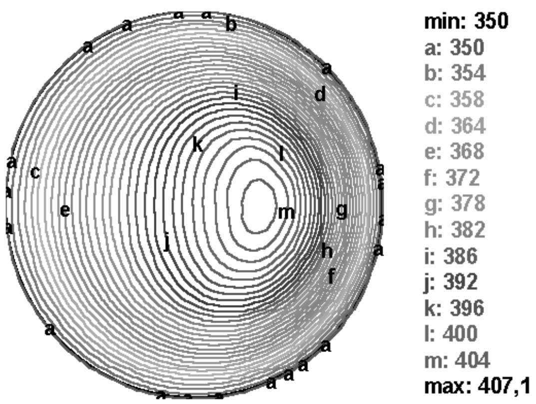

Figure 6a. Temperature contours (K) in the curved tube cross-section for *De* = 30

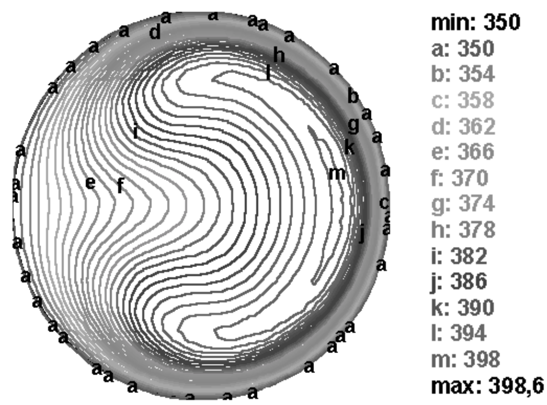

Figure 6b. Temperature contours (K) in the curved tube cross-section for *De* = 200

At small *De* number (Fig. 6a), the curvature effects are little accentuated and the fluid temperature maximum value is located near the tube central region. As the *De* number increases (Fig. 6b), the temperature field acquires an "inverted-C" configuration induced by the centrifugal force, with the temperature gradients (thermal boundary layer) more intense in the curved duct external wall.

Fig. 7 shows the dimensionless axial velocity at the curved tube cross-section (*De* = 30), under cooling and heating conditions in comparison with the isothermal flow ($\mu_{tb}/\mu_{tw} = 1$).

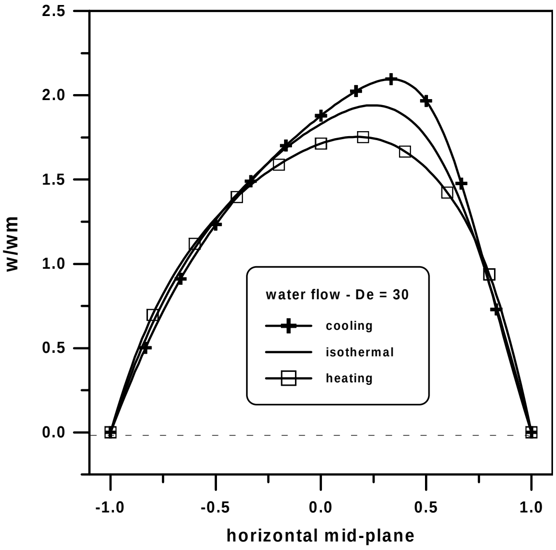

Figure 7a. Axial velocity profile at the horizontal mid-plane of the curved tube cross-section

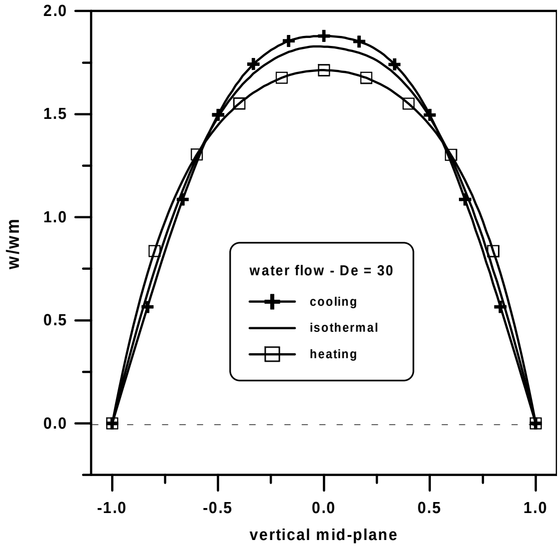

Figure 7b. Axial velocity profile at the vertical mid-plane of the curved tube cross-section

At the horizontal mid-plane, the axial velocity profile is displaced towards the duct external wall (Fig. 7a) due to the curvature effects, and this displacement is more accentuated in the water-cooling case. However, in the region close to the wall, the effect of the variable viscosity results in *w/wm* values is more intense under heating condition than in the cooling one.

At the vertical mid-plane distribution (Fig. 7b), the w/w_m profiles also exhibit higher values close to the wall and smaller at the central region of the curved duct when water is heated ($T_w > T_b$). Under cooling conditions ($T_w < T_b$) the influence of dependent-temperature viscosity is to increase the w/w_m values at the central region of the coil tube due to smaller viscosity values in this area.

Fig. 8 and Fig. 9 presents the temperature and viscosity distributions at the curved duct cross-section. At the horizontal mid-plane, Fig. 8a shows that the minimum (heating-water) and the maximum (cooling-water) temperature values are displaced towards the duct external wall because of the centrifugal force influence. As the viscosity depends on the temperature distributions, these curves also affect the viscosity profiles shown in Fig. 9a. When water is heated, appears a minimum value in the temperature profile (Fig. 8a) that is linked with a maximum in the viscosity distribution (Fig. 9a). Similarly, under cooling conditions ($T_w < T_b$ and $\mu_w > \mu_b$) the temperature exhibits a maximum (Fig. 8a) that is related with a minimum in the viscosity distribution. However, in the cooling-water case (Fig. 9a), the viscosity profile is smoother than the heating one due to the little temperature-varying viscosity shown in Fig. 2.

At the vertical mid-plane, Fig. 8b presents two minimum values in the temperature distribution under heating conditions ($T_w > T_b$ and $\mu_w < \mu_b$). Consequently, the viscosity variation profile for heating-water (Fig. 9b) is also more accentuated in comparison with the cooling one. This fact is due to a more intense gradient in the temperature-dependence viscosity (see Fig. 2).

Fig. 10a and Fig. 10b present the Nusselt number as a function of the Dean number for heating and cooling-water, respectively. By comparing, Fig. 4 and Fig. 10 it is verified that the *Nu* values obtained for the curved ducts are greater than the straight tube ones. This fact occurs because in the coil tube there is a increase in the momentum and energy transfers caused by the secondary flow (see Fig. 3b).

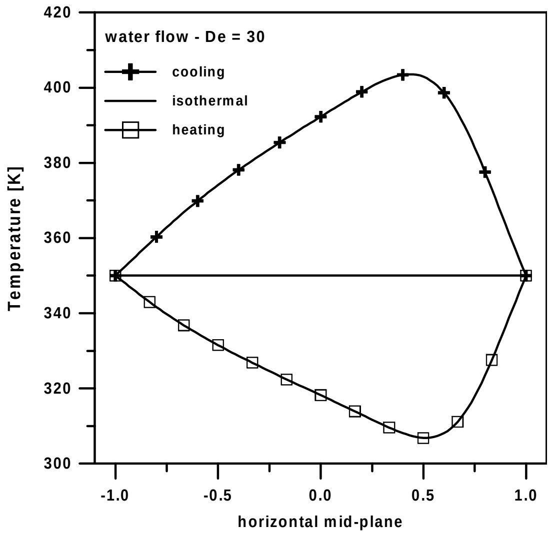

Figure 8a. Temperature distribution at the horizontal mid-plane of the tube cross-section

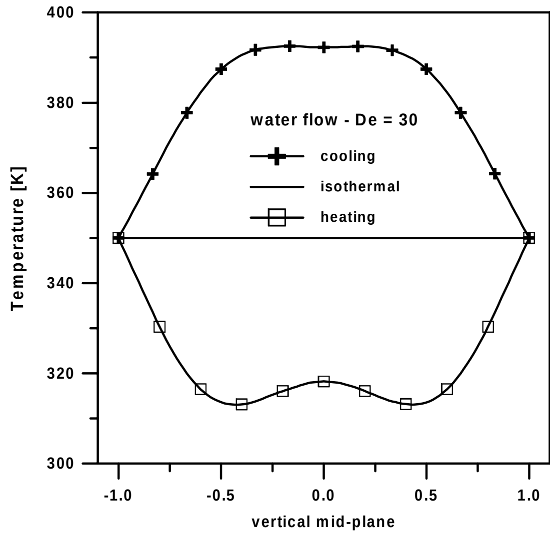

Figure 8b. Temperature distribution at the vertical mid-plane of the tube cross-section

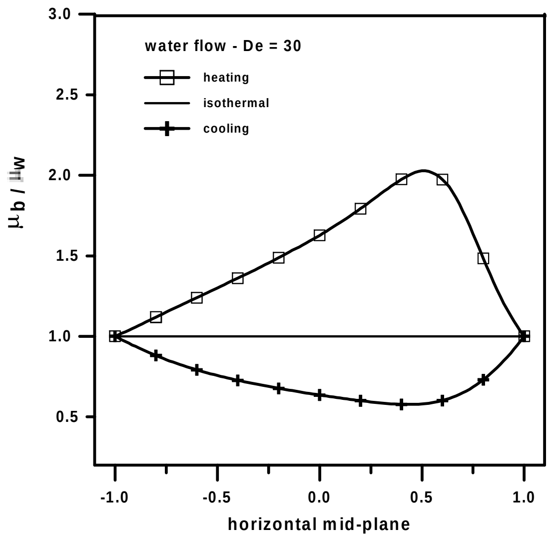

Figure 9a. Viscosity variation in the horizontal mid-plane of the curved tube cross-section

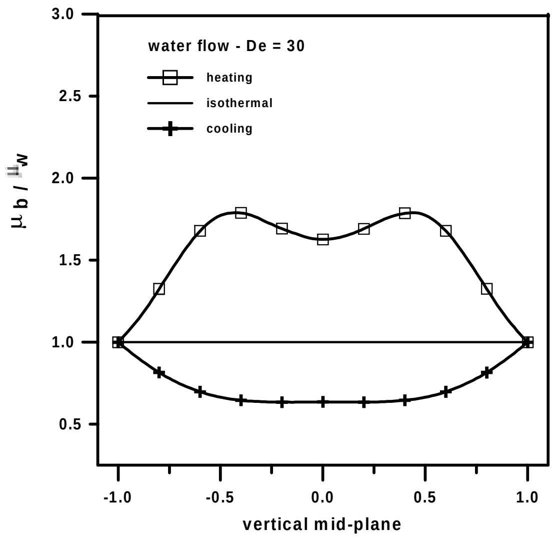

Figure 9b. Viscosity variation in the vertical mid-plane of the curved tube cross-section

It is also verified that the *Nu* values are higher in the heating-water (Fig. 10a) than in the cooling case (Fig. 10b), even if the viscosity variations aren't taken into account (constant-properties case corresponds to the dashed-line).

Besides, a comparison between the constant-properties and variable-viscosity results shows that under heating conditions the temperature-dependent viscosity assumption elevates the *Nu* value (Fig. 10a). On the other hand, when water is cooled, the Nusselt number is lower than the correspondent constant properties for all *De* number range analyzed. For example, this difference reaches almost 10%, at *De* = 80 (Fig. 10b). When the fluid is cooled considering variable-viscosity, the bulk mean temperature is lower than in the constant-viscosity case. This fact causes an increase of the viscosity values at the inner points of the curved tube section that reduces the secondary flow effect, and consequently the heat transfer rate.

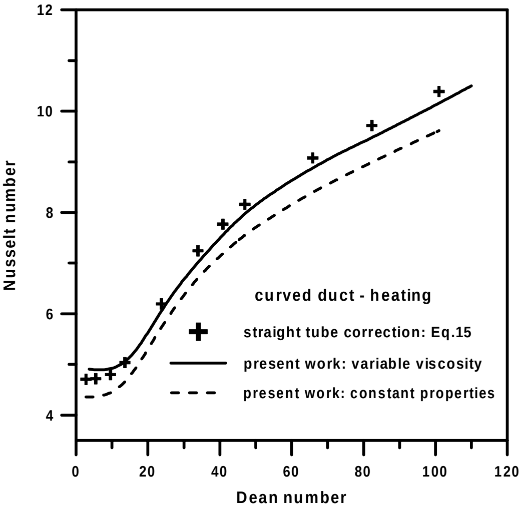

Figure 10a. Nusselt number as a function of the Dean number for heating-water

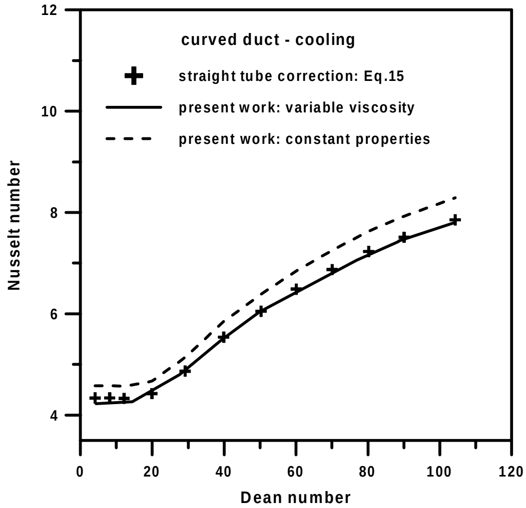

Figure 10b. Nusselt number as a function of the Dean number for cooling-water

Fig. 10 also shows the *Nu*-correction obtained from Eq. 15 (symbol-line in Fig. 10) with the necessary constant-properties Nu-values provided by the present work numerical data (dashed-line in Fig. 10). The property ratio method and the curved tube *Nu*-results are in good agreement in the cooling-water condition (Fig. 10b). In the heating case, however, the differences are more significant: the straight tube correction provides smaller *Nu*-values in comparison with the coil tube present work results (continuous-line in Fig. 10a) for $De < 20$. In the case of bigger *Dean* numbers the straight tube correction leads to overestimation when compared with the present study.

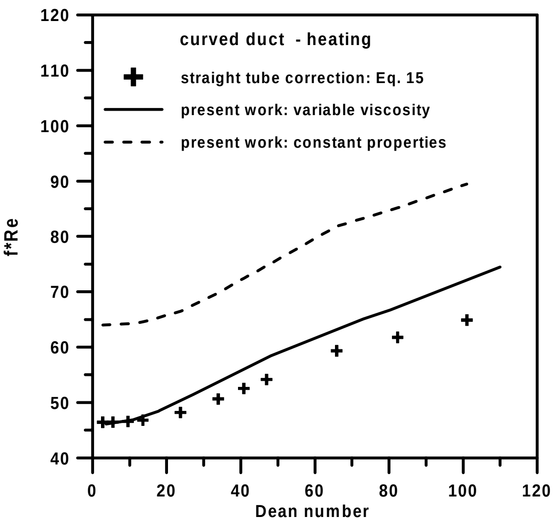

Figure 11a. Friction factor as a function of the Dean number for heating-water

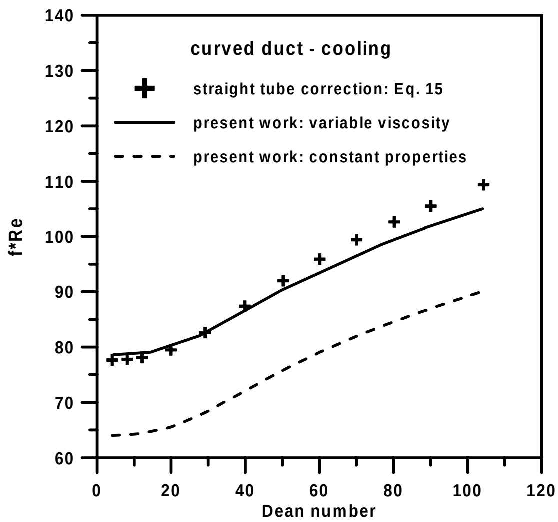

Figure 11b. Friction factor as a function of the Dean number for cooling-water

The *fRe* results for the curved duct are presented in Fig. 11. Under heating conditions (Fig. 11a) the variable-viscosity numerical data are lower than the constant-viscosity *fRe*-values. At this case, when the temperature-dependent viscosity is considered, the bulk mean temperature is greater than in the constant-properties case. This fact results in a lower viscosity that also reduces de friction factor in comparison with the constant-viscosity simulation. Nevertheless, when water is cooled, the *fRe* value with variable-viscosity is greater than the constant-properties ones, as shown in Fig.11b. This difference is more accentuated in the friction factor results than in the *Nu*-values (Fig. 10b), reaching 16% at *De* = 80 (Fig. 11b). Fig. 11 also presents the *fRe*-results based on the straight tube correction (Eq. 15 with *m* = -0,58 for heating and *m* = -0,50 for cooling case) for variable viscosity. Under both heating and cooling conditions, this method (symbol-line in fig. 11) exhibits a good agreement with the curved duct results (continuous line in Fig. 11) only for *De* < 20. As the Dean number increases, the property ratio method provides lower *fRe*-values (Fig. 11a) in comparison with the coil tube results. When water is cooled, the application of Eq. 15 overestimates the curved duct values (Fig. 11b).

5. CONCLUSIONS

A fully developed laminar water flow in a curved duct with temperature-dependent viscosity was analyzed under both heating and cooling conditions. The secondary flow induced by curvature effects increases the heat transfer rate in comparison with the straight ducts but the velocity and temperature profiles are distorted when the effects of temperature-varying viscosity are included. The Nusselt number and the friction factor results also show a marked dependence on the viscosity variations in the coil tube cross-section.

Under cooling conditions, the *Nu* values with variable-viscosity are lower than the constant-properties results due to the increase of the viscosity at the inner points of the curved tube section, that reduces the secondary flow effects and the heat transfer rate. The opposite case occurs when the water is heated.

Acknowledges

The authors are grateful to FAPESP, which supported this work (grant No. 99/03471-5).

REFERENCES

Bergles, A. E., 1983, "Prediction of the Effects of Temperature-Dependent Fluid Properties on Laminar Heat Transfer", *Low Reynolds Number Flow Heat Exchangers*, pp. 451-471.

Dean, W. R., 1927, "Note on the Motion of Fluid in a Curved Pipe", *Philosophical Magazine,* Series 7, vol. 4, pp. 208-223.

Etemad, S.GH., and Mujumdar, A.S. 1995, "Effects of Variable Viscosity and Viscous Dissipation on Laminar Convection Heat Transfer of a Power Law Fluid in the Entrance Region of a Semi-Circular Duct", *Int. J. Heat Mass Transfer,* Vol. 38, pp 2225-2238.

Harms, T. M., Jog, M. A. and Manglik, R. M. 1998," Effects of Temperature-Dependent Viscosity Variations and Boundary Conditions on Fully Developed Laminar Forced Convection in a Semicircular Duct", *Journal of Heat Transfer,* Vol. 120, pp 600-605.

Herwig, H., 1985, "The Effect of Variable Properties on Momentum and Heat Transfer in a Tube with Constant Heat Flux across the Wall", *Int. J. Heat Mass Transfer*, Vol. 28, pp 423-431.

Herwig, H. and Klemp, K. 1988, "Variable Property Effects of Fully Developed Laminar Flow in Concentric Annuli", *Journal of Heat Transfer*, Vol. 110, pp 314-320.

Incropera, F. P. and DeWitt, D. P. 1981, "*Fundamentals of Heat Transfer*", John Wiley & Sons, Inc. N.Y.

Kakaç, S. 1987, "The Effect of Temperature-Dependent Fluid Properties on Convective Heat Transfer", chap. 18 in *Handbook of Single-Phase Convective Heat Transfer"*, S. Kakaç, R.K. Shah and W. Aung, eds., John Wiley & Sons, Inc. N.Y.

Shah, R. K.and London, A. L., 1978, "Laminar Flow Forced Convection in Ducts", *Advances in Heat Transfer,* Academic Press.